PCCP

PAPER

View Article Online
View Journal | View Issue

Cite this: *Phys. Chem. Chem. Phys.*, 2021, **23**, 641

The effects of Feshbach resonance on spectral shifts in photoassociation of Cs atoms

Yuqing Li,[ab] Xiaofeng Wang,[a] Jizhou Wu,[ab] Guosheng Feng,[a] Wenliang Liu,[ab] Vladimir B. Sovkov,[c] Jie Ma,*[ab] Bimalendu Deb,*[d] Liantuan Xiao[ab] and Suotang Jia[ab]

Received 13th September 2020,
Accepted 27th November 2020

DOI: 10.1039/d0cp04840b

rsc.li/pccp

We study the effects of magnetic Feshbach resonance on the shifts in photoassociation (PA) spectra of ultracold Cs atoms. A series of atom loss spectra show a linear variation of the frequency shift with the PA laser intensity at different magnetic fields near the *d*-wave Feshbach resonance of optically trapped Cs atoms. The magnetic field-dependence of the slope of the shift on the PA laser intensity exhibits a dispersive change near the Feshbach resonance. The theoretical formula derived from a model based on Fano resonance fits well with the experimental data. Using a model rectangular potential with tunable well depth and applying the Franck–Condon principle, we obtain numerical results, which are found to be largely in disagreement with the experimental findings.

I. Introduction

Precision atom loss spectra in the photoassociation (PA) of ultracold atoms are important for determining the long-range coefficients of molecular potentials,[1,2] producing ultracold molecules[3] and altering the scattering length of colliding atoms by optical Feshbach resonance.[4] In PA spectra, the frequency of the resonance transition from ground atoms to excited molecules displays a shift with the increasing PA laser intensity, as experimentally demonstrated in the context of formation of molecules from atoms, including ultracold helium molecules $^4He_2$,[5] ultracold alkali molecule samples such as $^7Li_2$,[6–8] Na_2[9] and Cs_2,[10,11] and the heteronuclear molecule NaCs.[12] The PA spectral shifts have been calculated using the multichannel scattering theory.[13,14]

Magnetically controlled collisions of ultracold atoms in the presence of a PA laser have attracted increasing research interests.[15–17] It has been experimentally shown that the frequency shift in the PA spectra of ^{7}Li atoms has a strong dependence on the magnetic field near Feshbach resonance (FR) with an anomalous blueshift for the fields just below the FR.[8] The slope of the spectral shift in the PA of Cs atoms exhibits a linear variation when the magnetic field is tuned far away from FR.[11] A large number of studies have reported on the direct measurements of the spectral shift.[5–7,9,10,12] The precise control over the spectral shift by a magnetic field will provide more accurate information about the ultracold molecular rovibrational levels, opening a new perspective in the applications of PA spectral shifts.[18]

In this paper, the frequency shifts in PA spectra of optically trapped Cs atoms are measured in the vicinity of a *d*-wave Feshbach resonance. The variation of the slope of the PA spectral shift shows a dispersive curve with the magnetic field near the FR. This result shows that the FR can be used to control the spectral shift of PA. The experimental data can be well fitted by using the theoretical expression derived from the model of Fano resonance. Besides, the data are also analyzed by using the Franck–Condon principle involving a single channel rectangular potential with the tunable well depth. We find that the model based on Franck–Condon principle can not satisfactorily explain the observed data, while the model with Fano resonance shows quite good agreement with the experimental results.

II. Experimental setup

Cold Cs atoms are collected in a vapor-loaded magneto-optical trap (MOT), and then the compressed MOT and optical molasses are successively implemented to increase atomic density and lower atomic temperature. Afterwards, three-dimensional (3D) degenerated Raman sideband cooling (DRSC) is performed to spin polarize the atoms in the desired $F = 3$, $m_F = 3$ state and to lower the temperature of atoms to $\sim$1.7 μK. The low temperature obtained by the 3D DRSC prevents endothermic inelastic two-body collisions of Cs atoms in the $F = 3$, $m_F = 3$ state. As shown in Fig. 1, two

[a] State Key Laboratory of Quantum Optics and Quantum Optics Devices, Institute of Laser Spectroscopy, College of Physics and Electronics Engineering, Shanxi University, Taiyuan 030006, China. E-mail: mj@sxu.edu.cn
[b] Collaborative Innovation Center of Extreme Optics, Shanxi University, Taiyuan, Shanxi 030006, China
[c] St. Petersburg State University, 7/9 Universitetskaya nab., St. Petersburg 199034, Russia
[d] School of Physical Sciences, Indian Association for the Cultivation of Science, Jadavpur, Kolkata 700032, India. E-mail: msbd@iacs.res.in

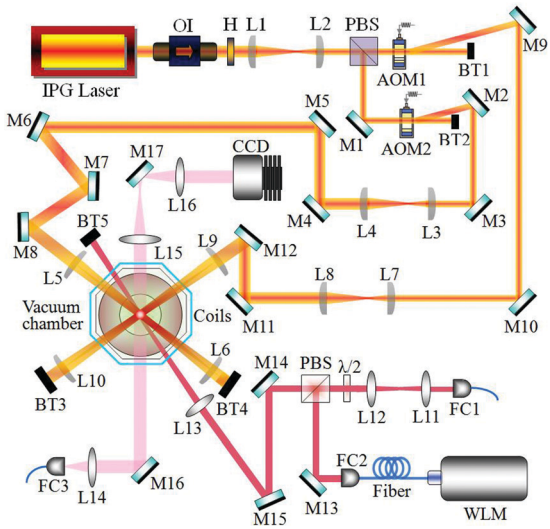

Fig. 1 Experimental geometry and configuration of lasers for investigating the effect of magnetic fields near a *d*-wave FR on the spectral shifts in PA of optically trapped ultracold Cs atoms. Two crossed dipole laser beams, PA laser and absorption image laser are overlapped at the center of the pairs of magnetic field coils. IPG, high power fiber laser; OI, optical isolator; H, half-wave plate; L, lens; PBS, polarization beam splitter; AOM, acousto-optic modulator; M, mirror; OF, optical fiber; FC, fiber coupler; BT, beam trap; WLM, wavelength meter; CCD, charge-coupled device.

horizontally crossing 1064 nm laser beams with the powers of 7 and 7.2 W at an angle of 90° are weakly focused on the trap center with the beam waists of ∼230 and 240 μm to form a crossed dipole trap, respectively. The cooled atomic sample is efficiently loaded into the optical dipole trap by applying the method of magnetic levitation, which is implemented by the application of both the magnetic field gradient of 31.3 G cm^{-1} and the bias field of 75 G.[19] The magnetic field gradient and the bias field are produced by a pair of quadrupole coils in an anti-Helmholtz configuration and a pair of bias coils in a Helmholtz configuration, respectively. We observe that the system approaches thermal equilibrium quite rapidly by the 500 ms plain evaporation at the bias field of 75 G.

To study the effect of the FR on the spectral shifts, the PA laser with a beam waist of 150 μm is switched on to illuminate the atomic cloud for 90 ms after tuning the magnetic field to the vicinity of the *d*-wave FR. The PA laser is provided by a widely tunable Ti:sapphire laser system and the frequency jitter is less than 500 kHz by locking to its self-reference cavity. The absolute frequency of PA laser is measured by a high-precision wavelength meter (HighFinesse WSU), which is repeatedly calibrated against the resonance transition frequency of the repumping laser at the beginning of each experimental cycle. The frequency of the PA laser is tuned near the resonance of the $v = 17$, $J = 0$ molecular rovibrational level of the Cs_2 0_g^- pure long-range state below the $6S_{1/2} + 6P_{3/2}$ dissociation limit.[20] PA resonances can be detected, because PA causes a reduction in atom number when excited molecules spontaneously decay into the ground molecules and the pairs of hot atoms that escape the trap. Before switching on the PA laser, the atomic density and temperature are 4×10^{11} cm^{-3} and 3.5 μK, respectively.

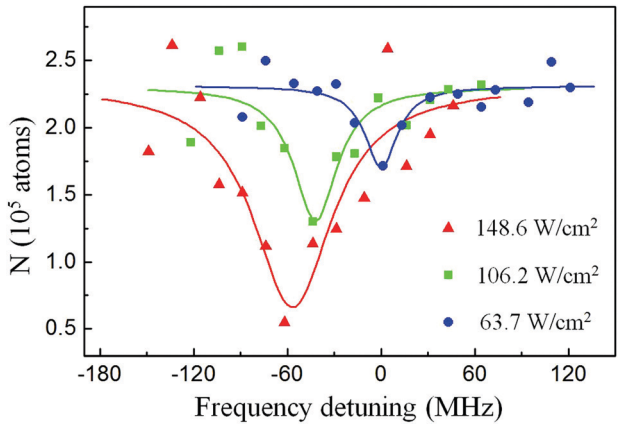

Fig. 2 PA spectra of the $v = 17$, $J = 0$ molecular rovibrational level of Cs_2 0_g^- pure long-range state for three different PA laser intensities of $I_{PA} = 63.7$ W cm^{-2} (blue circles), 106.2 W cm^{-2} (green squares) and 148.6 W cm^{-2} (red triangles) at the magnetic field of 47.731(5) G. The resonance location of PA is determined by fitting the data with a Lorentzian curve (solid curve). The spectral shift can be obtained by comparing the resonance positions at different PA laser intensities.

Fig. 2 shows the PA spectra, which are obtained by scanning PA laser frequency near 11681.9300 cm^{-1} with the PA laser intensities of $I_{PA} = 63.7$ W cm^{-2} (blue circles), 106.2 W cm^{-2} (green squares) and 148.6 W cm^{-2} (red triangles) at the magnetic field of 47.731(5) G. The atom loss reaches maximum when the frequency of the PA laser is tuned on the resonance transition to the excited molecules from the colliding ground atoms. The location of PA resonance at a particular intensity is determined by fitting the resonance line-shape to a Lorentzian curve. As the PA laser intensity is varied, the resonance position has an I_{PA}-induced shift. Additionally, the data clearly show that the increase of PA laser intensity induces the broadening of the linewidth of the PA resonance spectrum.

III. Experimental results

For ultracold Cs atoms in the $F = 3$, $m_F = 3$ state, there is a narrow *d*-wave FR, which alters the collisions of ultracold atoms by coupling the scattering atomic state to a bound *d*-wave molecular state.[21–23] The magnetic field is ramped from 75 G to the different final values near the FR within 30 ms. In Fig. 3, the variation of spectral shift with the intensity of PA laser is shown for six different magnetic fields, which are symmetrically chosen on both sides of the FR location. For a good signal-to-noise ratio of PA spectroscopy, we chose the PA laser intensity in the range from 63.7 W cm^{-2} to 169.9 W cm^{-2}. The observed linear dependence of spectral shift on the laser intensity is consistent with the calculation based on the multichannel scattering theory.[6,14] For the magnetic fields away from the FR, the spectral shifts show the variations with a similar slope. However, as the magnetic field increases and passes through the resonance location of the FR, the frequency shift shows a great change with the PA laser intensity. In other words, the FR has a great effect on the PA spectral shift.

The slope of spectral shift near the FR is derived by linear fitting of the variation of spectral shift with the PA laser intensity at

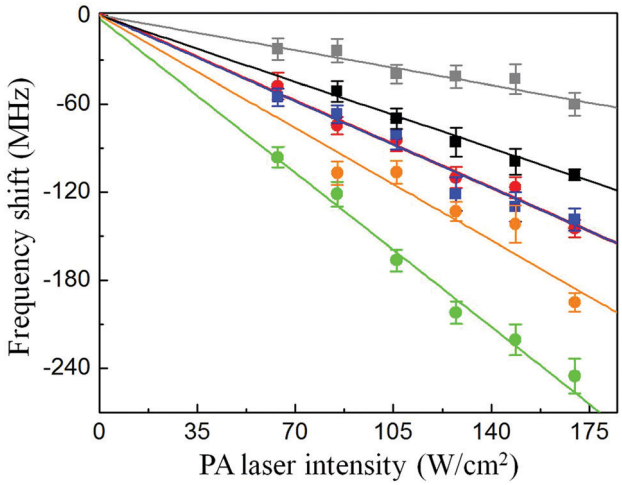

Fig. 3 The spectral shift as a function of the PA laser intensity for the v = 17, J = 0 molecular vibrational level of Cs_2 long-range 0_g^- state at magnetic fields of 47.731(5) G (red circles), 47.935 (orange circles), 47.986(5) G (green circles), 48.003(5) (gray squares), 48.037 (black squares) and 48.241(5) G (blue squares). The six magnetic fields are symmetrically chosen on both sides of the FR location to illustrate the non-monotonous influence of FR on the spectral shift. The colored solid lines represent linear fits to the corresponding experimental data.

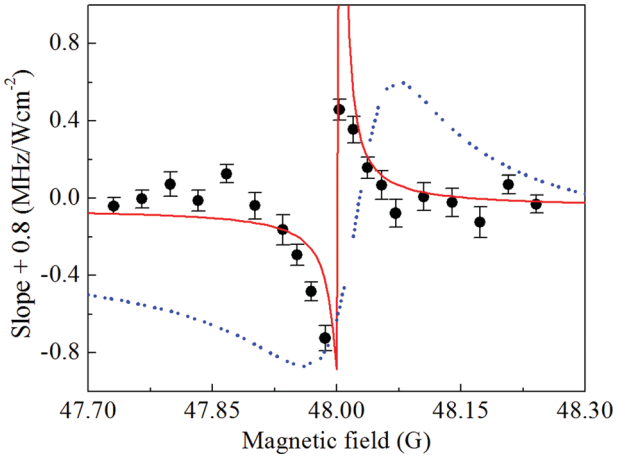

Fig. 4 Slope of the PA laser intensity-dependent spectral shift as a function of magnetic field near the FR. The red solid line is the fitted curve based on the model of Fano resonance. The theoretical fitting gives the Fano parameter of $q = -0.42 \pm 0.02$. The blue dashed line is obtained by the Franck–Condon principle considering the effect of external magnetic field on the scattering wavefunction of colliding atom pairs at a short interatomic separation at which the PA process may dominate.

different magnetic fields around the FR. As shown in Fig. 4, the FR has a significant effect on the slope of the frequency shift in PA spectra of ultracold Cs atoms. Far from the FR, the slope becomes a constant, which equals -0.8 MHz (W cm^{-2})$^{-1}$. As the magnetic field approaches the FR location from relatively low field, the amplitude of the slope of spectral shift below the FR becomes large. The amplitude of the slope of spectral shift decreases above the FR. In the experiment, the errors are mainly from the fitting error in determining PA resonant transition frequency, the error in measuring PA laser frequency, the systematic uncertainty induced by the fluctuation of the number of atoms prepared in each experimental cycle and the small uncertainties in controlling the magnetic field near the FR and measuring the intensity of PA laser.

IV. Model simulation

Here we discuss the model, which is used to explain the obtained experimental data. This model is based on an adaptation of Fano's theory[24,25] of continuum-bound coupled systems to the ultracold atom-molecule coupled systems. Though the model was presented in earlier works,[26] for the sake of completeness, we discuss the salient features of the model and reproduce some of the analytical results. In this model of Fano resonance, we consider that multiple bound states can be coupled to a continuum of states and there are bound–bound couplings as well. All the couplings including magnetic and optical couplings are treated on an equal footing, making the model suitable for nonperturbative calculations, which can result in a nonlinear Fano effect.[27]

Following Fano's theory, one can obtain a continuum-bound dressed state known as Fano state by diagonalizing the Hamiltonian involving one bound state interacting with a continuum of states. The well-known Beutler-Fano asymmetric spectral profile arises when optical dipole transitions occur between this Fano state and another bound state. In the linear Fano effect, the optical dipole coupling is treated perturbatively. As in Fano's theory, the theory of Feshbach resonance provides exact diagonalization of a continuum-bound coupled system. While Feshbach resonance normally refers to a scattering resonance, Fano resonance is a spectral resonance. However, both resonances can be treated with a unified approach of multichannel quantum scattering theory.[28]

In the present case, we have two bound states coupled to the continuum of atomic scattering states. In the absence of PA laser, the external magnetic field induces Feshbach resonance modeled by a simplified two-channel model in which one is open and the other is a closed channel. A quasi-bound state is supported by the closed channel. The PA laser couples both the quasi-bound state and the open-channel continuum states to an excited molecular bound state. We exactly diagonalize the system. The detailed calculations are given in the following derivation of spectral shift using the Fano model. The solution to the model provides analytical expression for nonperturbative spectral shift $\Delta E = S_q(B,E)\Gamma_{PA}$ where Γ_{PA} is the linewidth of PA spectrum in the absence of magnetic field and is a linear function of the laser intensity I_{PA} and

$$S_q(B,E) = \frac{1}{2}\left[\frac{(q^2-1)\beta - 2q}{\beta^2+1}\right]. \quad (1)$$

Here $S_q(B,E)$ is a dimensionless quantity that depends on the magnetic field B and the collision energy E but is independent of laser intensity I_{PA}. The dimensionless energy detuning parameter β is given by

$$\beta = \frac{E - E_c}{\Gamma_F/2}, \quad (2)$$

where E_c is the shifted binding energy of the quasi-bound molecular state $|b_c\rangle$ and Γ_F is the linewidth of magnetic Feshbach

resonance. So, the slope of the frequency shift to the laser intensity I_{PA}, that is, $\partial\Delta E/\partial I_{PA}$ is proportional to $S_q(B)$, which explicitly shows how the slope of the shift depends on the magnetic field and collision energy. Here q is the well-known Fano asymmetry parameter defined by

$$q = \frac{\Omega + V_{\text{eff}}}{\pi \Lambda_{\text{E}} V_{\text{E}}}, \tag{3}$$

where Ω is the bound–bound Rabi coupling, V_{eff} is the effective bound–bound coupling mediated by the continuum (for details, see the derivation of spectral shift using the Fano model), Λ_{E} is the PA laser-induced electric dipole coupling between the excited molecular bound state $|b_{\text{e}}\rangle$ and the continuum, while V_{E} is the coupling between the closed-channel quasi-bound state $|b_{\text{c}}\rangle$ and the continuum and is related to the linewidth of the Feshbach resonance by $\Gamma_{\text{F}} = 2\pi|V_{\text{E}}|^2$. When the magnetic field is tuned very close to the resonant magnetic field B_0, we have $E_{\text{c}} \simeq \delta\mu(B - B_{\text{c}})$,[22] where $\delta\mu$ is the difference between the magnetic moment of $|b_{\text{c}}\rangle$ and that of two free atoms in the continuum. Here B_{c} is the magnetic field at which the bare quasi-bound state $|b_{\text{c}}\rangle$ becomes degenerate with the entrance or open-channel threshold.

Our theory shows that the slope of the spectral shift is proportional to $S_{\text{q}}(B,E)$ of eqn (1). The proportional constant is denoted by $C = \Gamma_{\text{PA}}/I_{\text{PA}}$. At a fixed temperature which determines the collision energy E, $S_q(B,E)$ mainly depends on the magnetic field. So we fit this theoretical formula of $S = CS_q(B,E)$ with the parameters q and C. For the best fitting, we find $C = 9.58 \pm 0.75$ MHz (W cm^{-2})$^{-1}$ and $q = -0.42 \pm 0.02$. For the ultracold Cs atoms in the $F = 3$, $m_{\text{F}} = 3$ state, the parameters of the d-wave FR such as B_0, $\delta\mu$, Γ_{f} and B_{c} are given in ref. 22 and 23. As shown on the red line in Fig. 4, the fitting shows good agreement with experimental results. Since we found $-1 < q < 0$ from the fitting, we have $\Omega < |V_{\text{eff}}|$ according to the definition of q as given in eqn (3). Under the present physical conditions, this implies that the continuum-mediated bound–bound coupling V_{eff} dominates over the direct bound–bound coupling Ω as $V_{\text{eff}} < 0$ at low energy. The slope clearly shows the dispersive behavior, which can be described by the profile function $S_q(B,E)$. The variation of magnetic field leads to the variation of β, that is, the energy detuning due to the magnetic tuning of the open and closed channel thresholds. We here remark that our theory is a simplified model calculation.

Compared to the PA near a broad s-wave Feshbach resonance in ref. 8, our case shows the effect of a narrow d-wave Feshbach resonance on the PA. We use a different theoretical model, which is based on Fano resonance to explain our data and our theoretical result shows good agreement with experimental data. In ref. 8, the continuum-bound coupling dominates over the bound–bound coupling with the Fano asymmetry parameter $|q| > 1$,[29] while in our work the bound–bound coupling is significant and comparable with the continuum-bound coupling because in our work q is found to be $-1 < q < 1$.

Additionally, we verify whether the magnetic field-dependence of the slope of spectral shifts can be analyzed in terms of the Franck–Condon (FC) principle[6,14] and also the effect of external magnetic fields on the scattering wavefunction of colliding atom-pairs. According to the FC principle, PA predominately occurs at the Condon radius of $R_{\text{C}} \simeq 25.203$ Å.[20] A theoretical model with the depth-adjustable square potential is used to acquire the influence of external magnetic fields on the atomic scattering wavefunction in a short interatomic separation, in which the effective PA occurs.[30] As a result, the magnetic field-induced variation of the scattering length of colliding atoms[22] predominantly alters the atomic scattering wavefunction in the short interatomic separation (see the calculation based on FC principle). Although the calculation exhibits a tunable slope for the spectral shift near the FR, there is a large disagreement between the blue theoretical curve and the experimental data, as shown in Fig. 4. Previously the FC calculation with a depth-adjustable square potential was used to explain the variation of PA rate with the magnetic field far away from the FR location. However, the comparison of the theoretical calculation based on the FC principle to experimental data indicates that the FC calculation with a depth-adjustable square potential can not capture the physics when two coupled transitions are considered. The reasonable agreement between the Fano theory and the experimental data illustrates the coupling between the continuum-bound and bound–bound transitions.

V. Derivation of spectral shift using Fano model

The derivation of the shift of eqn (3) follows the same method as given in ref. 26. But, for the sake of completeness we here briefly discuss the method of derivation. Near the d-wave FR of Cs atoms, the atomic scattering state $|E\rangle$ is coupled to a quasi-bound d-wave molecular state $|b_{\text{c}}\rangle$ by the second order spin–orbit and spin–spin dipole interactions,[21,23] which are collectively modeled by the coupling parameter V_{E}. When the frequency of the PA laser is resonantly tuned to the transition from the state $|E\rangle$ to the state $|b_{\text{e}}\rangle$, the same PA laser induces an effective coupling between the states $|E\rangle$ and $|b_{\text{c}}\rangle$. V_{eff} is the continuum-mediated coupling between the bound states. To explain the measured atom loss, an artificial channel $|E''\rangle_{\text{art}}$ is introduced to mimic the decay of the excited molecular state $|b_{\text{e}}\rangle$[14,31] with the decay constant γ.

The Hamiltonian H_0 is given as

$$\begin{aligned} H_0 &= \int E\,\mathrm{d}E|E\rangle\langle E| - \hbar\delta|b_{\text{e}}\rangle\langle b_{\text{e}}| \\ &\quad + E_{\text{c}}|b_{\text{c}}\rangle\langle b_{\text{c}}| + \int E''\mathrm{d}E''|E''\rangle_{\text{art}}{}_{\text{art}}\langle E''| \end{aligned} \tag{4}$$

where δ is the detuning of the PA laser from the resonance transition from $|E\rangle$ to $|b_{\text{e}}\rangle$ and $|E''\rangle_{\text{art}}$ represents an artificial channel state. The interaction Hamiltonian H_{I} describing the couplings is given as

$$\begin{aligned} H_{\text{I}} &= \int \mathrm{d}E V_{\text{E}}|b_{\text{c}}\rangle\langle E| + \Omega|b_{\text{c}}\rangle\langle b_{\text{e}}| + \int \mathrm{d}E \Lambda_{\text{E}}|b_{\text{e}}\rangle\langle E| \\ &\quad + \int \mathrm{d}E'' V_{\text{art}}(E'')|b_{\text{e}}\rangle_{\text{art}}\langle E''| + \text{C.c.} \end{aligned} \tag{5}$$

where $V_{\text{art}}(E'')$ is a coupling between the artificial state $|E''\rangle_{\text{art}}$ and $|b_{\text{e}}\rangle$. The Hamiltonian $H = H_0 + H_{\text{I}}$ can be diagonalized using the Fano's method as in ref. 26 and 29, yielding a dressed

continuum state, which is a coherent superposition of the states $|E\rangle$, $|b_c\rangle$, $|b_e\rangle$ and $|E''\rangle_{art}$. We can thus obtain the analytical expressions for the expansion coefficients of all states in the dressed continuum. Among these four expansion coefficients, the expansion coefficient A_E of the state $|b_e\rangle$ is important for describing the PA-induced atom loss, which is given by the probability of transition from the dressed continuum to the artificial channel. Explicitly,

$$A_E = \frac{(q+\beta)/(\beta+i)\Lambda_E}{\tilde{\delta} - \Delta E + i\hbar(\gamma + \Gamma_q)} \tag{6}$$

where

$$\Gamma_q = \frac{(q+\beta)^2}{\beta^2+1}\Gamma_{PA} \tag{7}$$

and $\tilde{\delta} = \hbar\delta - E^0_{shift}$ with E^0_{shift} being the PA shift of $|b_e\rangle$ in the absence of a magnetic field. Here $\Delta E = S_q(B,E)\Gamma_{PA}$ are the magnetic field- and energy-dependent spectral shifts where $S_q(B,E)$ is given by eqn (1). The Fano asymmetry parameter q can be obtained as a fitting parameter. In the experiment, we have a certain colliding energy determined by the atomic temperature and so the $S_q(B,E)$ is mainly dependent on the magnetic field.

VI. Calculation based on the Franck–Condon principle

We also carry out calculations based on the FC principle to see whether this can explain the observed slope of PA spectral shift. Here we use the theoretical expression of the frequency shift as given in ref. 6 and 14. The frequency shift is proportional to the product of the PA laser intensity and the overlap integral between the wavefunctions of the atomic scattering state and the excited molecular state. According to the FC principle, PA mainly occurs at the Condon radius, and the slope of frequency shift is proportional to the FC overlap integral $\langle b_e|E\rangle$. The wavefunction $|b_e\rangle$ is calculated using the potential curve of excited Cs molecules.[32] About the atomic wavefunction, we need to achieve the theoretical dependence of atomic wavefunction on the magnetic field near the FR. Multichannel calculations of magnetic FR, using up-to-date and high-precision molecular potential data from Cs_2, require at least 24 hyperfine channels to obtain agreement with the observed magnetic FR.[21] Instead of the extremely complicated multichannel calculations, we use a single-channel square potential with the tunable potential depth, which was proposed and tested in ref. 22 and 33, to simulate the scattering behavior of Cs atoms near the d-wave FR. Considering the threshold behavior of atomic scattering state under the van der Waals interaction, the size of the square well, which is used to calculate the continuum state $|E\rangle$, is taken to be the mean scattering length $\bar{a} = 95.7a_0$.[22,30] For $r > \bar{a}$, the scattering wavefunction is $\phi_E(r) = \sqrt{\frac{k}{\pi E}}\sin(kr+\eta)$, where $E = \frac{h^2k^2}{2m_r}$ is the collision energy. The scattering phase shift η is given by $\cot\eta = -1/(ak) + r_0k/2$, where a is the s-wave scattering length and r_0 is the effective range. For $r \le \bar{a}$, $\phi_E(r) = A\sin(k'r)$, where the parameters A and k' can be derived using the scattering boundary condition at $r = \bar{a}$. When the magnetic field is tuned near the FR, the wavefunction $\phi_E(r)$ for $r > \bar{a}$ varies with η. According to the requirement of the continuous boundary condition, the wavefunction for $r \le \bar{a}$ changes with the variable k', which is dependent on the depth of the square potential. As a result, the slope of frequency shift shows a variation near the FR. The theoretical calculation of the slope of frequency shift is shown in Fig. 4. Compared to the theoretical result based on the model of Fano resonance, there is a large disagreement between the theory based on the FC principle and the experiment.

VII. Conclusions

In conclusion, we have investigated the effect of the d-wave magnetic FR on the spectral shift for the PA resonance of optically trapped ultracold Cs atoms. The slope of spectral shift to the PA laser intensity shows a dispersive variation as a function of magnetic field across the FR location. The theoretical formula derived from the model of Fano resonance is fitted on the observed dependence of the slope on the magnetic field near the FR, and the theory shows good agreement with the experiment. A model calculation based on FC principle was also carried out by using a single channel rectangular potential with a tunable well depth, which is introduced to acquire the influence of the magnetic field on the atomic scattering wavefunction in the effective PA range. Compared to the model of Fano resonance, the calculation based on the FC principle seems to be inadequate to account for the experimental data. A particularly interesting aspect of our study is the narrow dispersive behavior of the slope of PA spectral shift, which can be well explained by the model of nonlinear or non-perturbative Fano resonance. The d-wave Feshbach resonance used for our study has a very narrow width. Accordingly, Fano dip, which occurs due to quantum interference-induced dark resonance, has a narrow width.[34] Since Fano minimum implies reduction of absorption or enhanced transparency, it might be an interesting study to explore the effects of dispersive slope of PA spectral shift on the propagation of light through Fano-resonant ultracold atomic medium.

Author contributions

Y. L., X. W., G. F., and W. L. peformed the experiments. J. W., V. S. and J. M. supervised the experimental work. B. D. contributed theoretical analysis. All authors contributed to the analysis and discussions of the results and the preparation of the manuscript.

Conflicts of interest

There are no conflicts to declare.

Acknowledgements

The National Key Research and Development Program of China (Grant No. 2017YFA0304203), the National Natural Science Foundation of China (Grant No. 61722507, 61675121, 61705123, and

61901249), PCSIRT (No. IRT17R70), STIP, the Program for the Outstanding Innovative Teams of Higher Learning Institutions of Shanxi (OIT), the Applied Basic Research Project of Shanxi Province, China (Grant No. 201901D211191, and 201901D211188), the collaborative grant by RFBR and NNSF of China (No. 2053-53025), and the Open Research Fund Program of the State Key Laboratory of Low-Dimensional Quantum Physics, are acknowledged.

Notes and references

1 M. Pichler, H. Chen and W. C. Stwalley, *J. Chem. Phys.*, 2004, **121**, 1796.
2 J. Ma, Y. Q. Li, W. L. Liu, P. Chen, G. S. Feng, C. Y. Hu, J. Z. Wu, L. T. Xiao and S. T. Jia, *Opt. Express*, 2014, **22**, 3756.
3 K.-K. Ni, S. Ospelkaus, M. H. G. de Miranda, A. Pe'er, B. Neyenhuis, J. J. Zirbel, S. Kotochigova, P. S. Julienne, D. S. Jin and J. Ye, *Science*, 2014, **322**, 231.
4 M. Theis, G. Thalhammer, K. Winkler, M. Hellwig, G. Ruff, R. Grimm and J. H. Denschlag, *Phys. Rev. Lett.*, 2004, **93**, 123001.
5 M. Portier, S. Moal, J. Kim, M. Leduc, C. CohenTannoudji and O. Dulieu, *J. Phys. B.*, 2006, **39**, S881.
6 J. M. Gerton, B. J. Frew and R. G. Hulet, *Phys. Rev. A: At., Mol., Opt. Phys.*, 2001, **64**, 053410.
7 I. D. Prodan, M. Pichler, M. Junker, R. G. Hulet and J. L. Bohn, *Phys. Rev. Lett.*, 2003, **91**, 080402.
8 M. Junker, D. Dries, C. Welford, J. Hitchcock, Y. P. Chen and R. G. Hulet, *Phys. Rev. Lett.*, 2008, **101**, 060406.
9 C. McKenzie, J. H. Denschlag, H. Häffner, A. Browaeys, L. E. E. de Araujo, F. K. Fatemi, K. M. Jones, J. E. Simsarian, D. Cho, A. Simoni, E. Tiesinga, P. S. Julienne, K. Helmerson, P. D. Lett, S. L. Rolston and W. D. Phillips, *Phys. Rev. Lett.*, 2002, **88**, 120403.
10 J. Z. Wu, Z. H. Ji, Y. C. Zhang, L. R. Wang, Y. T. Zhao, J. Ma, L. T. Xiao and S. T. Jia, *Opt. Lett.*, 2011, **36**, 2038.
11 Y. Q. Li, G. S. Feng, W. L. Liu, J. Z. Wu, J. Ma, L. T. Xiao and S. T. Jia, *Opt. Lett.*, 2015, **40**, 2241.
12 W. L. Liu, X. F. Wang, J. Z. Wu, X. L. Su, S. Wang, V. B. Sovkov, J. Ma, L. T. Xiao and S. T. Jia, *Phys. Rev. A: At., Mol., Opt. Phys.*, 2017, **96**, 022504.
13 P. O. Fedichev, Y. Kagan, G. V. Shlyapnikov and J. T. M. Walraven, *Phys. Rev. Lett.*, 1996, **77**, 2913.
14 J. L. Bohn and P. S. Julienne, *Phys. Rev. A: At., Mol., Opt. Phys.*, 1999, **60**, 414.
15 B. L. Tolra, N. Hoang, B. T'Jampens, N. Vanhaecke, C. Drag, A. Crubellier, D. Comparat and P. Pillet, *Europhys. Lett.*, 2003, **64**, 171.
16 P. Pellegrini, M. Gacesa and R. Côté, *Phys. Rev. Lett.*, 2008, **101**, 053201.
17 S. P. Krzyzewski, T. G. Akin, J. Dizikes, M. A. Morrison and E. R. I. Abraham, *Phys. Rev. A: At., Mol., Opt. Phys.*, 2015, **92**, 062714.
18 K. M. Jones, E. Tiesinga, P. D. Lett and P. S. Julienne, *Rev. Mod. Phys.*, 2006, **78**, 483.
19 Y. Q. Li, G. S. Feng, R. D. Xu, X. F. Wang, J. Z. Wu, G. Chen, X. C. Dai, J. Ma, L. T. Xiao and S. T. Jia, *Phys. Rev. A: At., Mol., Opt. Phys.*, 2015, **91**, 053604.
20 A. Fioretti, D. Comparat, C. Drag, C. Amiot, O. Dulieua, F. Masnou-Seeuws and P. Pillet, *Eur. Phys. J. D*, 1999, **5**, 389.
21 C. Chin, V. Vuletić, A. J. Kerman, S. Chu, E. Tiesinga, P. J. Leo and C. J. Williams, *Phys. Rev. A: At., Mol., Opt. Phys.*, 2004, **70**, 032701.
22 A. D. Lange, K. Pilch, A. Prantner, F. Ferlaino, B. Engeser, H.-C. Nägerl, R. Grimm and C. Chin, *Phys. Rev. A: At., Mol., Opt. Phys.*, 2009, **79**, 013622.
23 C. Chin, R. Grimm, P. S. Julienne and E. Tiesinga, *Rev. Mod. Phys.*, 2010, **82**, 1225.
24 U. Fano, *Phys. Rev.*, 1961, **124**, 1866.
25 A. E. Miroshnichenko, S. Flach and Y. S. Kivshar, *Rev. Mod. Phys.*, 2010, **82**, 2257.
26 B. Deb, *J. Phys. B.*, 2010, **43**, 085208.
27 M. Kroner, A. O. Govorov, S. Remi, B. Biedermann, S. Seidl, A. Badolato, P. M. Petroff, W. Zhang, R. Barbour, B. D. Gerardot, R. J. Warburton and K. Karrai, *Nature*, 2008, **451**, 311.
28 J. P. Connerade, *Highly excited atoms*, Cambridge University Press, 1998.
29 B. Deb and G. S. Agarwal, *J. Phys. B.*, 2009, **42**, 215203.
30 G. S. Feng, Y. Q. Li, X. F. Wang, J. Z. Wu, V. B. Sovkov, J. Ma, L. T. Xiao and S. T. Jia, *Sci. Rep.*, 2017, **7**, 13677.
31 Y. Q. Li, G. S. Feng, J. Z. Wu, J. Ma, B. Deb, A. Pal, L. T. Xiao and S. T. Jia, *Phys. Rev. A: At., Mol., Opt. Phys.*, 2019, **99**, 022702.
32 N. Bouloufa, A. Crubellier and O. Dulieu, *Phys. Rev. A: At., Mol., Opt. Phys.*, 2007, **75**, 052501.
33 C. Chin, arXiv:cond-mat., 2005, 0506313.
34 S. Moal, M. Portier, J. Kim, J. Dugué, U. D. Rapol, M. Leduc and C. Cohen-Tannoudji, *Phys. Rev. Lett.*, 2006, **96**, 023203.

